RSC Advances

ROYAL SOCIETY OF CHEMISTRY

www.rsc.org/advances

Novel hybrid micro-supercapacitor based on conducting polymer coated silicon nanowires for electrochemical energy storage

David Aradilla,[a,b] Gérard Bidan,[c] Pascal Gentile,[b*] Patrick Weathers,[a] Fleur Thissandier,[a,b] Vanesa Ruiz,[d] Pedro Gómez-Romero,[d] Thomas J. S. Schubert,[e] Hülya Sahin,[e] and Saïd Sadki[a*]

[a]LEMOH/SPrAM/UMR 5819 (CEA,CNRS, UJF), CEA/INAC Grenoble, France

[b]SiNaPS Lab.-SP2M, UMR-E CEA/UJF, CEA/INAC Grenoble, France

[c]INAC/Dir, CEA/INAC Grenoble, 17 rue des Martyrs, 38054-Grenoble, France

[d]ICN2 (CSIC-ICN). Campus UAB. 08193 Bellaterra, Barcelona, Spain

[e]IOLITEC Ionic Liquids Technologies GmbH, Salzstrasse 184, 74076 Heilbronn, Germany

*Corresponding authors: pascal.gentile@cea.fr and said.sadki@cea.fr

The development of a novel hybrid symmetric micro-supercapacitor based on poly(3,4-ethylenedioxythiophene) coated silicon nanowires using an ionic liquid (N-methyl-N-propylpyrrolidinium bis(trifluoromethylsulfonyl)imide) as an electrolyte has been demonstrated. The hybrid supercapacitor device was able to deliver a specific energy of 10 Wh kg^{-1} and a maximal power density of 85 kW kg^{-1} at a cell voltage of 1.5 V. The hybrid device exhibited long lifetime and an outstanding electrochemical stability retaining 80 % of the initial capacitance after thousands of galvanostatic charge-discharge cycles at a high current density of 1 mA cm^{-2}. The improvement of the capacitive properties compared with the bare SiNWs was attributed to the pseudo-capacitive behavior induced by the conducting polymer coating.

1. Introduction

Conjugated organics polymers have awakened a great interest in the field of polymer science due to its interesting electrical, electrochemical and optical properties.[1] The structure and chemical nature of π-conjugated polymers (CPs) have allowed the development of technological devices in a wide range of applications such as sensors (e.g. biosensors or electrochemical sensors),[2,3] biomedical engineering,[4] electrochromic devices,[5] photovoltaic cells,[6] and supercapacitors.[7,8] Poly(3,4-ethylenedioxythiophene) (PEDOT) is considered as one of the most important CPs owing to its excellent properties in terms of high conductivity, high electro-activity, low oxidation potential and good electrochemical stability.[9,10] According to these features, PEDOT has been widely developed in the field of energy storage, specifically in supercapacitors based on active carbon,[11] graphene,[12] carbon nanotubes,[13] or carbon fiber.[14] Within this context, supercapacitors can be categorized into two main groups regarding their working principle: (1) electrochemical double layer capacitors (EDLCs), which store energy by electrostatic charge accumulation at electrode/electrolyte interfaces, and (2) pseudo-capacitors where the mechanism of charge storage is based on faradaic or redox reactions associated with charge transfer processes, which occur at the surface of the electrodes. In general terms, pseudo-capacitors have shown better results in terms of specific capacitance than EDCLs, which have attracted a special attention in the field of electrochemical energy storage devices. Nowadays, pseudo-capacitive materials for supercapacitors include mainly conducting polymers (e.g. polythiophene, polypyrrole, polyaniline or their derivatives) and transition metal oxides (e.g. RuO_2 or MnO_2).[15]

In recent years, the development of new supercapacitors known as micro-supercapacitors or micro-ultracapacitors has aroused a special attention due to their possible integration into miniaturized portable electronic devices such as micro-electromechanical systems (MEMS) or micro-robots, which could supply micro power sources for energy harvesting.[16] Currently, tremendous efforts have been devoted to improve the performance and properties of micro-supercapacitors using nanostructured carbon materials (e.g. onion-like carbon).[17] In spite of the improvements achieved combining nanostructured materials with different device architectures and configurations (e.g. interdigital structures), the development of high performance micro-supercapacitors is still a challenge. Over the past years, silicon nanowires (SiNWs) grown by chemical vapor deposition have attracted a great attention as micro-

supercapacitor electrodes according to its interesting capacitive properties in terms of pulse power capabilities and long cycle life. Additionally, nanostructured silicon electrodes could be easily integrated in the Si-based microelectronics industry which represents an advantage to micro-supercapacitor electrodes based on carbon. Thus, SiNWs in a 2-electrode configuration were studied in different electrolytes as for example organic solvents (a propylene carbonate solution containing 1M tetraethylammonium tetrafluoroborate)[18-21] or ionic liquids (1-ethyl-3-methylimidazolium bis(trifluoromethylsulfonyl)imide, EMIM TFSI)[22] showing an excellent capacitive behavior for micro-supercapacitors. In order to improve the capacitive properties in terms of specific capacitance, power and energy densities of EDLCs based on SiNWs, the development of new pseudocapacitive materials-based electrodes is still in progress. Currently, different strategies have already been reported by using metallic oxides (NiO)[23,24] or cermets (SiC)[25] for the coating of SiNWs to be employed as supercapacitor electrodes. To the best of our knowledge only one work has been reported dealing with the deposition of conducting polymer onto SiNWs (e.g. electrochemical deposition of a PEDOT coating employing an acetonitrile solution containing 0.1 M lithium perchlorate) for electrochemical energy storage devices, which was employed in the field of Li ion batteries with the aim of improving their cycling stability.[26] In this work, we report the first preliminary study of the performance of symmetric hybrid PEDOT coated SiNWs micro-supercapacitors in a sandwich type configuration using N-methyl-N-propylpyrrolidinium bis(trifluoromethylsulfonyl)imide (PYR_{13} TFSI) ionic liquid as electrolyte. Nowadays, the use of ionic liquids has been employed as alternative electrolytes in different energy applications (e.g. supercapacitors)[27] regarding their wide electrochemical window (>4V) and high thermal stability (> 300°C).[28] Moreover, the electrochemical deposition of PEDOT was carried out by means of potentiostatic methods using also a PYR_{13} TFSI solution as the polymerizing medium and as a dopant, which allowed the electropolymerization of PEDOT at a low oxidation potential. The electrochemical characterization of the hybrid device was evaluated by using cyclic voltammetry, galvanostatic charge-discharge cycles and electrochemical impedance spectroscopy using a cell voltage of 1.5 V. A morphological characterization of the SiNWs was examined by using scanning and transmission electron microscopies before and after the cycling galvanostatic test.

2. Experimental

Materials and reagents. Highly n-doped Si (111) substrates (doping level: $5 \cdot 10^{18}$ doping atoms cm^{-3}) and resistivity less than 0.005 Ω cm were used as the substrate for SiNW growth. Gold colloid solution (50 nm) was purchased from British BioCell. 3,4-ethylenedioxythiophene and silver trifluoromethanesulfonate were purchased from Sigma-Aldrich. N-methyl-N-propylpyrrolidinium bis(trifluoromethylsulfonyl)imide was purchased from IOLITEC (Ionic Liquids Technologies GmbH, Germany) and used without further purification.

Growth of SiNWs. SiNWs electrodes with a length of approximately 15 μm and a diameter of 50 nm were grown in a CVD reactor (EasyTube3000 First Nano, a Division of CVD Equipment Corporation) by using the vapor-liquid-solid (VLS) method via gold catalysis on highly doped n-Si (111) substrate. Gold colloids with size of 50 nm were used as catalysts, H_2 as carrier gas, silane (SiH_4) as silicon precursor, phosphine (PH_3) as n-doping gas and HCl as additive gas. The use of HCl has been proved to reduce the gold surface migration and improve the morphology of SiNWs.[29,30] Prior to the growth, wafer surface was cleaned by successive dipping in acetone, isopropanol and Caro (H_2SO_4:H_2O_2, 3:1 v/v) solutions in order to remove organic impurities, after that, the substrates were dipped in HF 10% and NH_4F solution to remove the native oxide layer. Finally, the gold catalyst was deposited on the surface. The deposition was carried out using HF 10 % from an aqueous gold colloid solution.

The growth was performed at 600°C, under 6 Torr total pressure, with 40 sccm (standard cubic centimeters) of SiH_4, 100 sccm of PH_3 gas (0.2% PH_3 in H_2), 100 sccm of HCl gas and 700 sccm of H_2 as supporting gas. The doping level (dl) of the SiNWs was managed by the pressure ratio: dopant gas / SiH_4, which was evaluated in previous works (dl : $4 \cdot 10^{19}$ cm^{-3}).[29]

Electropolymerization of EDOT on SiNWs. PEDOT films were electrochemically deposited from a PYR_{13} TFSI solution containing 0.1 M EDOT as the monomer using an AUTOLAB PGSTAT 302 N potentiostat-galvanostat. The electropolymerization was conducted in a 3-electrode electrochemical cell. SiNWs were employed as the working electrode, a Pt wire was used as the counter electrode and the nonaqueous Ag/Ag^+ reference electrode was composed of a silver wire immersed in a 10 mM silver trifluoromethanesulfonate (AgTf) solution in PYR_{13} TFSI. The electrochemical deposition of PEDOT was carried out by potentiostatic methods using a constant

potential of 0.4 V (vs Ag/Ag^+) under a polymerization charge of 750 mC cm^{-2} controlled by the chronocoulometry technique in an argon-filled glove box with oxygen and water levels less than 1 ppm. After the electrochemical deposition the electrodes were washed in acetone and dried with a N_2 flow before the electrochemical characterization. The PEDOT mass was estimated by substracting the difference before and after electrodeposition on SiNWs using a METTLER Toledo balance (precision of 0.01 mg). A total mass of $2.5 \cdot 10^{-4}$ g was identified for each electrode.

Design of the hybrid micro-supercapacitor. Symmetric micro-supercapacitors were designed from hybrid nanostructured electrodes made of PEDOT-coated SiNWs as mentioned in the previous section. A homemade two-electrode supercapacitor cell was built by assembling two hybrid nanostructured electrodes separated by a Whatman glass fiber paper separator soaked with the electrolyte (PYR_{13} TFSI).

Electrochemical characterization of micro-supercapacitors. Cyclic voltammetry (CV) and galvanostatic charge - discharge curves were performed between 0 and 1.5 V using different scan rates (0.02 - 0.3 Vs^{-1}) and current densities (0.1 - 1 mA cm^{-2}) respectively. Electrochemical impedance spectroscopy (EIS) measurements were performed using a sinusoidal signal of ±10 mV amplitude and a frequency range from 100 kHz to 10 mHz. Electrochemical tests were performed using a multichannel VMP3 potentiostat/galvanostat with Ec-Lab software (Biologic, France). All measurements were carried out using PYR_{13} TFSI as electrolyte in an argon-filled glove box with oxygen and water levels less than 1 ppm at room temperature.

Morphological characterization. The morphology of the resulting SiNWs before and after electrochemical testing was examined by using a ZEISS Ultra 55 scanning electron microscope operating at an accelerating voltage of 3 kV and a JEOL 3010 transmission electron microscopy at an accelerating voltage of 300 kV. The elements distribution of the PEDOT-coated SiNWs was probed by energy-dispersive X-ray spectrometry (EDX) element mapping analysis at a voltage of 6 kV. SiNWs were rinsed with acetone and isopropanol to ensure removal of excess electrolyte after electrochemical testing.

Results and discussion

The morphology of the bare SiNWs and PEDOT coated SiNWs was characterized by SEM. Figure 1a shows the SEM image of the resulting SiNWs after the growth by using the VLS method described in the methods section. The morphology

reflects a high density of nanowires with the gold colloids kept on the top of the SiNWs with a diameter of 50 nm. The density of nanowires was estimated to be ~10^8 nanowires cm^{-2} as reported in previous works.[19,20] Figure 1b displays the surface morphology after the PEDOT deposition. As can be seen, a uniform and homogeneous PEDOT coating on the surface of the SiNWs proved the success of the electrochemical deposition based on potentiostatic methods. The cross-sectional view shown in Figure 1c allowed an estimation of the length of the PEDOT-coated SiNWs of approximately 15 µm, which was corroborated according to the Figure 1a. Figure 1d shows that the surface of PEDOT on SiNWs presents a granular agglomerated structure forming small clusters. According to Figure 1d, the PEDOT-coated SiNWs shows a total thickness of 352 nm, whereas the PEDOT layer was estimated to be about 300 nm thick. TEM was used to examine and confirm the coating of PEDOT onto SiNWs as illustrated in Figure 1d. The corresponding EDX elemental maps were carried out in order to investigate the element distribution in the hybrid SiNWs. As shown in Figure 1f, the obtained images show distributions of Si and S. Thus, Si is located on SiNWs whereas S corresponds to the chemical structure of PEDOT. In overall, SEM, TEM and EDX results confirm that the electrochemically polymerized PEDOT uniformly covers the SiNWs.

Figure 2a shows cyclic voltammograms of the SiNWs-PEDOT symmetric supercapacitor at various scan rates. As can be seen, all CVs show near rectangular shape indicating a highly capacitive behavior. The shape of the curves is retained even at a relatively high scan rate of 300 mV/s indicating good reversibility in the electrode/electrolyte interface. Regarding Figure 2a, the capacitive current increased linearly with the sweep rate reflecting good rate capability at high charge-discharge rates and a negligible ohmic drop in the electrolyte bulk. Figure 2b represents the impedance spectra plots of the PEDOT coated SiNWs micro-supercapacitors. The Nyquist plot reflects a semi-circle in the high frequency range and a vertical line in the low frequency range (insert Figure 2b). The diameter of the high frequency arc is denoted as the charge transfer resistance (R_{CT}) which determines the rate at which the supercapacitor can be charged and discharged. Thus, an ionic resistance value of 43 Ω cm^{-2} was calculated according to the inset in Figure 2b. Another important characteristic of the impedance spectra is associated with the equivalent series resistance (ESR) obtained from the intersection with the real axis (Z') at the high frequency region corresponding to zero for Z''. This parameter is a very important factor in order to determine the maximal power density (P^{max}) of a micro-supercapacitor according to the

following equation (P^{max}: V^2 / 4ESR) where V is the cell potential. Thus, the ESR was calculated to be 26.40 Ω cm^2 (Inset Figure 2b) which leads to a P^{max} value of 85.20 kW kg^{-1}. The low values of R_{CT} (43 Ω cm^{-2}) and ESR (27 Ω cm^{-2}) indicate a fast and high electrolyte penetration on the hybrid electrodes. At the low frequency range a slope of a nearly vertical line arise due to the faradaic pseudo-capacitance of the PEDOT coating on the SiNWs. The vertical line reflected at low frequency indicates also a limiting electrolyte diffusion process, which displays a pure capacitive behavior and relatively fast ion diffusion in the electrodes. The charge-discharge profiles of the hybrid symmetric micro-supercapacitor using different density currents are illustrated in Figure 2c. The discharge curves are almost linear and symmetric in the potential range of 1.5 V indicating an excellent capacitive behaviour. The specific capacitance of the hybrid micro-supercapacitor was calculated from the profiles displayed in Figure 2c using the following equation:

$$SC = \frac{I\,\Delta t}{\Delta V m} \qquad (1)$$

where SC (F g^{-1}) is the specific capacitance of the hybrid micro-supercapacitor, I (A) corresponds to the discharge current, ΔV (V) is the potential change within the discharge time Δt (s), and m (g) refers to the PEDOT mass of one electrode per cm^2. As shown in Figure 2d, a specific capacitance value of ~36 F g^{-1} (~9 mF cm^{-2}) was calculated at a current density of 0.1 mA cm^{-2}, and a value of 32 F g^{-1} (~8 mF cm^{-2}) at a current density of 1 mA cm^{-2}. In the literature, micro-supercapacitors using conducting polymer microelectrodes (e.g. polypyrrole or poly-(3-phenylthiophene)) on silicon substrates have been reported with a cell capacitance value ranging from 1.6 up to 14 mF.[31] The values of specific capacitance obtained in this study using were found also to be in the same order of magnitude than those based on symmetric redox supercapacitors made from MEMS technologies.[32] Those symmetric supercapacitors consisted of a three-dimensional (3D) microstructure on a silicon substrate and two electrochemically polymerized polypyrrole (PPy) films as electrodes exhibited a specific capacitance of 56 mF cm^{-2}. More recently, the same configuration of PPy electrodes on symmetric micro-supercapacitor with 3D interdigital electrodes designed and fabricated through carbon MEMS technology reflected a value of 78 mF cm^{-2}.[33] On the other hand, it is worth noting that the hybrid redox symmetric micro-supercapacitors assembled in this work have shown better results in terms of specific capacitance (~ 8-9 mF cm^{-2}) than

interdigitated on-chip micro-supercapacitors based on carbide derived carbon films (e.g. SC: 1.5 mF cm^{-2}),[34] or onion-like carbon based micro-supercapacitor electrodes prepared by electrophoretic deposition (e.g. SC: 1.1 mF cm^{-2}).[35] The results highlight that PEDOT-coated SiNWs micro-supercapacitors exhibit higher specific capacitance values than carbon-based micro-ultracapacitors with interdigital in-plane architectures.[36] Additionally, micro-supercapacitors based on PEDOT-coated SiNWs showed values in terms of specific capacitance larger than bare SiNWs micro-supercapacitors[18] (e.g. values ranging from 10 to 51 μF cm^{-2}). This tendency corroborates the synergistic effect induced by the conducting polymer coating for micro-supercapacitors based on nanostructured silicon electrodes.

The Ragone plot in Figure 3 reflects the energy density (E, Wh kg^{-1}) and average power density (P, kW kg^{-1}) of PEDOT-coated SiNWs micro-supercapacitors according to the following equations:

$$E = \frac{1}{2} SC\Delta V^2 \quad (2)$$

$$P = \frac{E}{\Delta t} \quad (3)$$

The Ragone plot increases rapidly with power density due to the fast voltage decay during discharge as shown in Figure 3. At a current density of 1 mA cm^{-2} the hybrid device exhibited a specific energy and power density value of 10 Wh kg^{-1}(~9 mJ cm^{-2}) and 3.3 kW kg^{-1} (~0.8 mW cm^{-2}). Power density and specific energy were ranged from 0.3 up to 3.3 kW kg^{-1} and from 10.1 up to 11.4 Wh kg^{-1} respectively. These values were found to be larger than those found for micro-supercapacitors based on PPy electrodes using MEMS technologies, thus power density values of 0.56 mW cm^{-2} and 0.63 mW cm^{-2} were recently reported in literature.[32,33] Again, the performance of hybrid SiNWs-PEDOT micro-supercapacitors reflect the improvement of the capacitive properties in terms of specific capacitance and energy compared with other redox micro-supercapacitors (e.g. PPy electrodes), or bare SiNWs micro-supercapacitors.[18]

The long-term stability of the hybrid device was investigated by applying a large number of galvanostatic charge-discharge cycles at a current density of 1 mA cm^{-2} between 0 and 1.5 V. As can be seen in Figure 4a a gradual decrease of the specific capacitance was observed. Thus, a loss of specific capacitance of approximately 20% was found after 3500 galvanostatic cycles. This value was compared with other micro-supercapacitors based on pseudo-capacitive electrode materials reflecting a remarkable

electrochemical stability for the hybrid device based on PEDOT-coated SiNWs. Thus, micro-supercapacitors based on nanostructured MnO_2 electrodes onto Si wafers showed a loss of ~27 % after 1000 galvanostatic cycles.[37] On the other hand, the coulombic efficiency (η) defined as the ratio between the discharge and charge time was observed during the cycling with a value of ~ 99 % showing the effective reversibility of the PEDOT-SiNWs hybrid device. The morphology of the PEDOT-coated SiNWs after cycling was examined by using SEM images according to Figure 4b. As illustrated, the structure of PEDOT-coated SiNWs remained unchanged even after thousands of successive charge-discharge cycles presenting no degradation at the structural level of the morphology, thus, comparable to those observed in Figure 1b and 1c corresponding to PEDOT-coated SiNWs as grown (e.g. not cycled in an electrochemical device).

The electrochemical deposition of PEDOT coating on SiNWs has demonstrated an amazing improvement of the capacitive properties due to the pseudo-capacitive behavior of the conducting polymer compared with bare SiNWs. The synergistic effect between the PEDOT and SiNWs concludes that hybrid micro-supercapacitors can be employed as alternatives to carbon-based EDLCs in the Si-based microelectronics industry.

3. Conclusions

The electrochemical deposition of PEDOT on SiNWs using potentiostatic methods has been successfully proven in the presence of PYR_{13} TFSI. The hybrid symmetric PEDOT-coated SiNWs micro-supercapacitor performed in PYR_{13} TFSI, as the ionic liquid electrolyte, showed an excellent performance in terms of maximal power density (85 kW kg^{-1}), specific energy (10 Wh kg^{-1}) and specific capacitance (32 F g^{-1}). The hybrid device showed an outstanding and remarkable electrochemical stability with a loss of specific capacitance of 20% after 3500 charge-discharge galvanostatic cycles. This work represents the first study of the performance of hybrid symmetric micro-supercapacitors based on SiNWs with conducting polymer. The results of this study were compared with those from micro-supercapacitors based on nanostructured carbon electrodes and conducting polymer demonstrating the excellent performance of PEDOT-coated SiNWs micro-supercapacitors in terms of capacitance, power density and energy. Therefore, this type of hybrid supercapacitor can be considered as a new prospective electrochemical energy storage device for its integration and miniaturization into micro-electronic devices in the near future.

Acknowledgements

The authors acknowledge the CEA for financial support of this work. This project has received funding from the European Union's Seventh Programme for research, technological development and demonstration under grant agreement No 309143 (2012 – 2015). Authors are thankful to Dr. Danet for his kind assistance in TEM studies.

References

1 A. G. MacDiarmid, "Synthetic Metals": A Novel Role for Organic Polymers (Nobel Lecture). *Angew. Chem. Int. Ed.* 2001, **40**, 2581 – 2590.

2 M.Gerard, A. Chaubey and B. D. Malhotra, *Biosens. Bioelectro.*, 2002, **17**, 345 – 359.

3 G. Bidan, *Sens. Actuat. B* 1992, **6**, 45 – 56.

4 R. Ravichandran, S. Sundarrajan, J. R. Venugopal, S. Mukherjee and S. Ramakrishna, *J. R. Soc. Interface* 2010, **7**, S559 – S579.

5 P. M. Beaujuge and J. R. Reynolds, *Chem. Rev.*, 2010, **110**, 268 – 320.

6 A. Fachetti, *Chem. Mater.*, 2011, **23**, 733 – 758.

7 G. A. Snook, P. Kao, and A. S. Best, *J. Power Sources* 2011, **196**, 1 – 12.

8 R. Ramya, R. Sivasubramanian and M. V. Sangaranarayanan, *Electrochim. Acta* 2013, **101**, 109 – 129.

9 L. B. Groenendaal, F. Jonas, D. Freitag, H. Pielartzik and J. R. Reynolds, *Adv. Mater.*, 2010, **12**, 481 – 494.

10 S. Kirchmeyer, and K. Reuter, *J. Mater. Chem.*, 2005, **15**, 2077 – 2088.

11 C. Lei, P. Wilson and C. Lekakou, *J. Power Sources* 2011, **196**, 7823 – 7827.

12 J. Zhang and X. S. Zhao, *J. Phys. Chem. C* 2012, **116**, 5420 – 5426.

13 J. Chen, C. Jia and Z. Wan, *Electrochim. Acta* 2014, **121**, 49 – 56.

14 G. P. Pandey, A. C. Rastogi and C. R. Westgate, *J. Power Sources* 2014, **245**, 857 – 865.

15 G. Xiong, C. Meng, R. G. Reifenberger, P. P. Irazoqui, and T. S. Fisher, *Electroanalysis* 2014, **26**, 30 – 51.

16 D. R. Rolison, J. W. Long, J. C. Lytle, A. E. Fischer, C. P. Rhodes, T. M. McEvoy, M. E. Bourg and A. M. Lubers, *Chem. Soc. Rev.*, 2009, **38**, 226 – 252.

17 D. Pech, M. Brunet, H. Durou, P. Huang, V. Mochalin, Y. Gogotsi, P.-L. Taberna and P. Simon, *Nat. Technol.*, 2010, **5**, 651 – 654.

18 F. Thissandier, P. Gentile, N. Pauc, E. Hadji, A. Le Comte, O. Crosnier, G. Bidan, S. Sadki and T. Brousse, *Electrochemistry* 2013, **81**, 777 – 782.

19 F. Thissandier, A. Le Comte, O. Crosnier, P. Gentile, G. Bidan, E. Hadji, T. Brousse and S. Sadki, *Electrochem. Commun.*, 2012, **25**, 109 – 111.

20 F. Thissandier, N. Pauc, T. Brousse, P. Gentile and S. Sadki, *Nanoscale Research Lett.*, 2013, **8**, 38 – 42.

21 J. W. Choi, J. McDonough, S. Jeong, J. S. Yoo, C. K. Chan, and Y. Cui, *Nano Lett.*, 2010, **10,** 1409 – 1413.

22 F. Thissandier, L. Dupré, P. Gentile, T. Brousse, G. Bidan, D. Buttard and S. Sadki, *Electrochim. Acta* 2014, **117**, 159 – 163.

23 B. Tao, J. Zhang, F. Miao, S. Hui and L. Wan, *Electrochim. Acta* 2010, **55**, 5258 – 5262.

24 F. Lu, M. Qiu, X. Qi, L. Yang, J. Yin, G. Hao, X. Feng, J. Li and J. Zhong, *Appl. Phys. A* 2011, **104**, 545 – 550.

25 J. P. Alper, M. Vincent, C. Carraro and R. Maboudian, *Appl. Phys. Lett.*, 2012, **100**, 163901 – 163904.

26 Y. Yao, N. Liu, M. T. McDowell, M. Pasta and Y. Cui, *Energy Environ. Sci.*, 2012, **5**, 7927 – 7930.

27 D. R. MacFarlane, N. Tachikawa, M. Forsyth, J. M. Pringle, P. C. Howlett, G. D. Elliott, J. H. Davis, M. Watanabe, P. Simon and A. Angell, *Energy Environ. Sci.*, 2014, **7**, 232 – 250.

28 M. Armand, F. Endres, D. R. MacFarlane, H. Ohno and B. Scrosati, *Nat. Mater.*, 2009, **8**, 621 – 629.

29 P. Gentile, A. Solanki, N. Pauc, F. Oehler, B. Salem, G. Rosaz, T. Baron, M. Den Hertog and V. Calvo, *Nanotechnology* 2012, **23**, 215702 – 215707.

30 F. Oehler, P. Gentile, T. Baron and P. Ferret, *Nanotechnology* 2009, **20**, 475307 – 475312.

31 J.-H. Sung, S.-J. Kim and K.-H. Lee, *J. Power Sources* 2003, **124**, 343 - 350.

32 W. Sun, R. Zheng and X. Chen, *J. Power Sources* 2010, **195**, 7120 – 7125.

33 M. Beidaghi and C. Wang, *Electrochim. Acta* 2011, **56**, 9508 – 9514.

34 P. Huang, M. Heon, D. Pech, M. Brunet, P.-L. Taberna, Y. Gogotsi, S. Lofland, J. D. Hettinger and P. Simon, *J. Power Sources* 2013, **225**, 240 – 244.

35 P. Huang, D. Pech, R. Lin, J. K. McDonough, M. Brunet, P.-L. Taberna, Y. Gogotsi and P. Simon, *Electrochem. Commun.*, 2013, **36**, 53 – 56.

36 M. Beidaghi and Y. Gogotsi, *Energy Environ. Sci.*, 2014, **7**, 867 – 884.

37 X. Wang, B. D. Myers, J. Yan, G. Shekhawat, V. Dravid and P. S. Lee, *Nanoscale* 2013, **5**, 4119 – 4122.

Captions to Figures

Figure 1. (a) Cross sectional view of SiNWs. (b) SEM image of PEDOT coated SiNWs at 45° tilted angle. (c) Cross sectional view of PEDOT coated SiNWs. (d) Cross sectional view of an individual PEDOT coated SiNW. The SiNW is marked with an asterisk whereas the PEDOT coating is indicated with an arrow. (e) TEM micrograph of PEDOT coated SiNWs. (f) EDX maps of Si and S onto PEDOT-coated SiNWs. Inset reflects the distribution of Si corresponding only to SiNWs.

Figure 2. Characterization of SiNWs / PEDOT micro-supercapacitors. (a) Cyclic voltammograms at different scan rates (0.02, 0.05, 0.075, 0.1, 0.2 and 0.3 Vs^{-1} respectively). Arrow indicates the increase of scan rate. (b) Nyquist plot measured at 0V. The impedance was measured using a frequency range from 100 kHz to 10 mHz. Inset shows an enlarged scale of the impedance spectra in the origin. (c) Charge - discharge curves recorded at different current densities (0.1, 0.25, 0.50, 0.75 and 1 mA cm^{-2} respectively). (d) Specific capacitance versus current density.

Figure 3. The Ragone plot for a SiNWs / PEDOT micro-supercapacitor calculated by varying the discharging current density of 0.1 to 1 mA cm^{-2}.

Figure 4. (a) Lifetime testing of the SiNWs / PEDOT micro-supercapacitors performed using 3500 complete charge - discharge cycles at a current density of 1 mA cm^{-2} between 0 and 1.5 V. (b) SEM micrographs of PEDOT coated SiNWs after cycling under the conditions described in a) at 45° tilted angle.

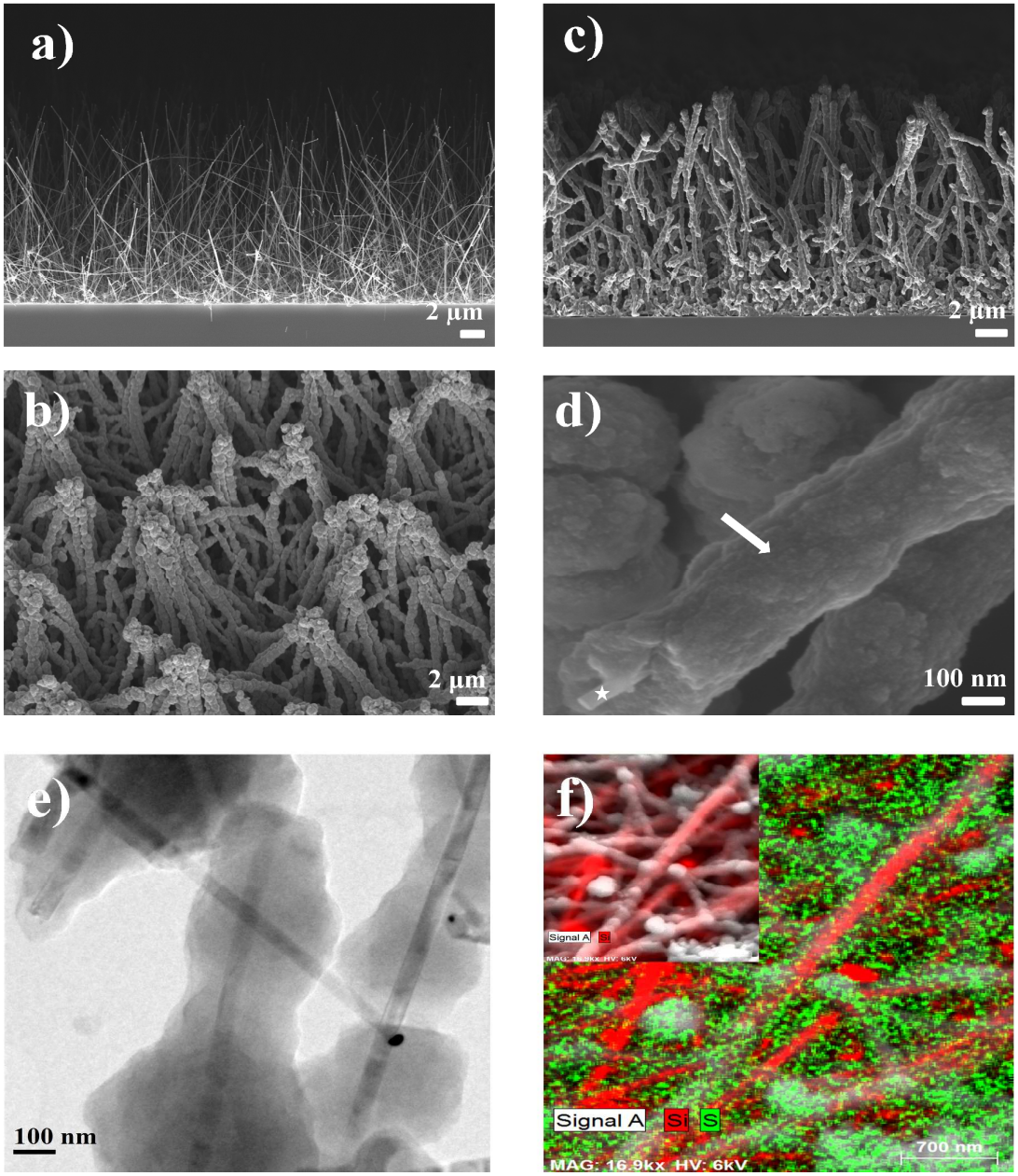

Figure 1

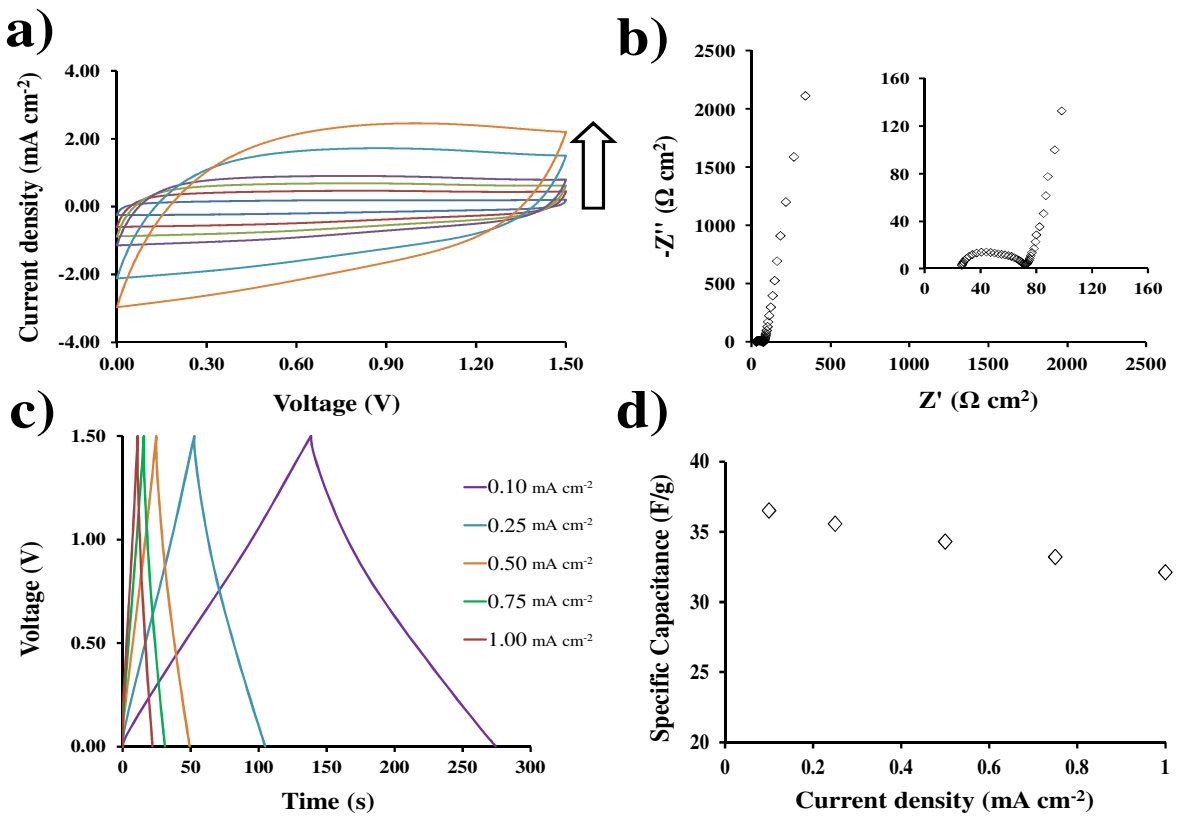

Figure 2

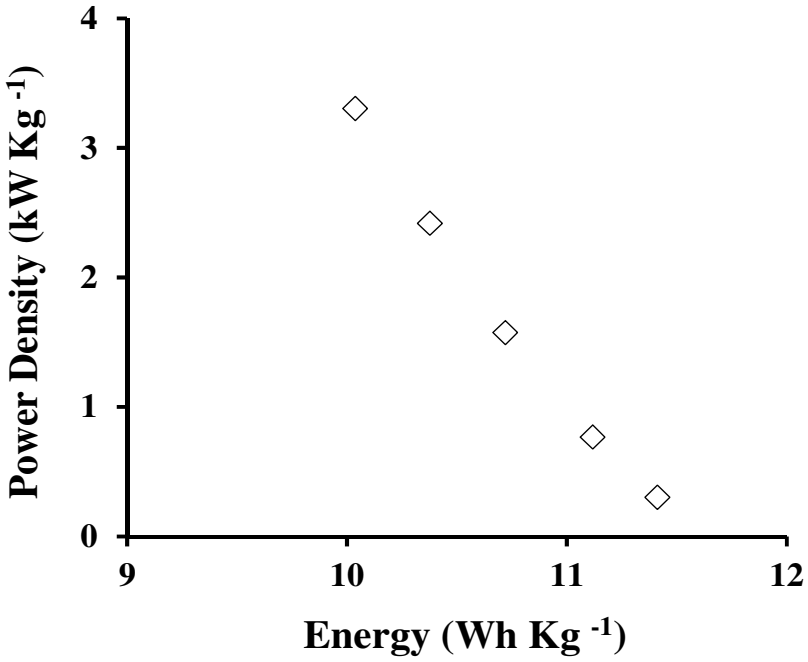

Figure 3

a)

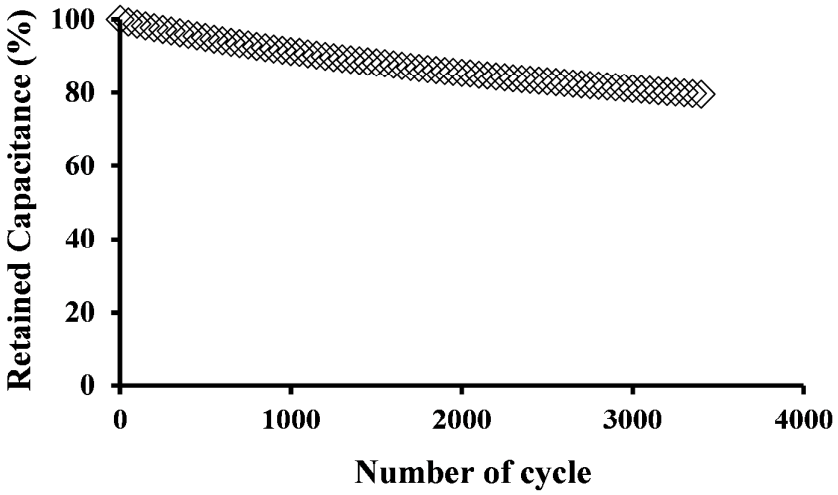

b)

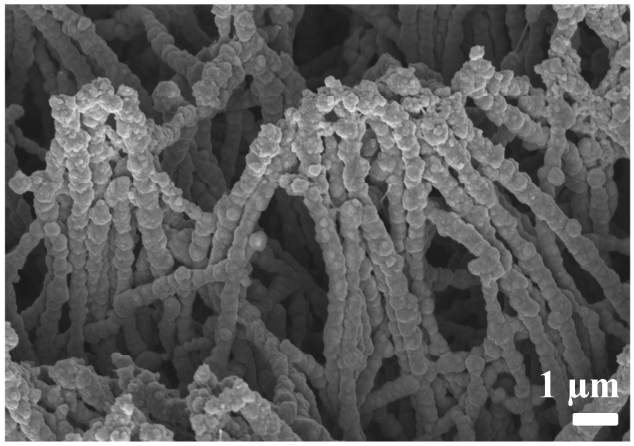

Figure 4